P. M. McGuiggan

S. M. Hsu

Ceramics Division,
National Institute of Standards and Technology,
Gaithersburg, MD 20899

W. Fong

D. Bogy

U. C. Berkeley,
Computer Mechanics Lab,
Berkeley, CA 94702

C. S. Bhatia

Storage Systems Division,
IBM Corporation,
San Jose, CA 95193

Friction Measurements of Ultra-Thin Carbon Overcoats in Air

The friction force as a function of humidity was measured between thin carbon films coated onto mica surfaces. The friction force was found to be proportional to the area of contact. The shear stress at 0 percent, 33 percent, and 100 percent relative humidity was measured to be 26 MPa±5 MPa, *12* MPa±2 MPa, *and 5* MPa±0.5 MPa, *respectively, and was independent of the applied pressure for pressures less than 20 MPa. Water acts as a lubricant decreasing the friction between the carbon surfaces. The shear stress at 0 percent relative humidity corresponds to the shear stress of a solid paraffin film, and suggests that the shear may be dominated by a thin organic film adsorbed from air, at least at the pressures less than 20 MPa and a velocity of 1 μm/s. At 100 percent relative humidity, the shear stress for carbon coated surfaces was about double that for mica surfaces, indicating a stronger influence of the water for the more hydrophilic mica surface than the more hydrophobic carbon surface. The friction between one uncoated mica and one carbon coated mica surface resulted in immediate damage and generation of wear debris.* [DOI: 10.1115/1.1387035]

Introduction

Amorphous carbon films are commonly used as protective overcoats in magnetic hard disks [1–3]. The properties of these overcoats include high wear resistance, high hardness, low friction coefficients, and high corrosion resistance [1,4–16]. Each of these properties is crucial for proper protection of the magnetic hard disk. The need to provide adequate protection of the hard disk by keeping the head and disk separated is in conflict with the need to increase storage capacities by decreasing the spacing between the head and the recording material. Because of the strict requirement for small spacing, carbon overcoat thicknesses as low as 5 nanometers are currently being used.

A variety of techniques have been used to study the microstructure and mechanical and tribological properties of nanometer thick films [1,4–25]. The results from the various techniques are dependent upon the underlying substrates, the atmospheric conditions, and the structure and chemistry of the films [3,4,7,8]. Specifically, friction is often determined by an interfacial (tribochemical) transfer film which may form during solid-solid sliding, and not by the bulk properties of the materials that constitute the surfaces or films [7,18]. The measured friction force is related to the interfilm sliding between the transfer film and the original surface. Often, the transfer film is chemically distinct from the parent film [18].

Three forms of carbon—graphite, diamond, and diamond-like carbon (amorphous carbon, a-C)—are currently being studied for low friction surfaces [1,4–16,18,22–25]. Each form of carbon shows dramatically different chemical and friction properties under various environmental conditions [8,11,14–16,18,21,22,24–28]. For example, an increase in dangling bonds may occur on diamond surfaces in vacuum, thereby increasing the friction force [15]. Also, the form of the carbon may change with sliding. An increase in the graphite content of the carbon has been proposed to occur with sliding [24,26].

Besides the chemistry and form of the carbon, atmospheric conditions may dictate the behavior of the material. Surface reactions such as oxidation may occur, and the rate of the reaction is greatly increased during rubbing [15,18,22,26]. Besides oxidative effects, humidity plays an important role [13,14,16,18,19,21,22,27,28]. For self-mating materials, i.e., where carbon is slid against carbon, some researchers have shown the friction force to increase with humidity whereas other researchers have shown a decrease with humidity [16,18]. When steel or Si_3N_4 is slid against amorphous carbon, the friction coefficient generally increases as the humidity increases [14,22,25], although some studies find little change [27]. Hydrogen-free amorphous carbon is less susceptible to humidity than hydrogenated amorphous carbon [8]. As opposed to amorphous carbon, the friction force generally decreases with humidity for graphite and diamond materials [18].

The aim of this work is to investigate the tribological properties of two amorphous carbon films slid laterally against each other as a function of humidity using the Surface Forces Apparatus (SFA) [19,20,29,30].[1] We are measuring in a low applied pressure regime (<20 MPa) and hence we expect little wear to occur. Using the SFA technique, the contact area can be measured and wear can be visualized when it occurs. We chose to measure the friction force in dry and humid air because these conditions are important in many industrial applications. We observed that the friction force decreases with increasing humidity. This decrease in the friction force cannot be explained by a decrease in adhesion, indicating that water acts as a lubricant between the surfaces. Results are also presented of the sliding of one carbon-coated surface against an uncoated mica surface where immediate damage of the mica surface occurred.

Experimental Procedure

I Surface Preparation. Muscovite mica was cleaved to a few micrometer thickness and cut into sheets 1 cm^2. Approximately 50 nm silver was evaporated onto the back of the mica sheet. The mica surface was then glued, silver side down, onto a silica disk using a hot melt epoxy. The thin amorphous carbon films were deposited directly onto the molecularly smooth mica surfaces by magnetron sputtering with a graphite target according to the procedure described by Lu and Komvopoulos [4]. The mica surfaces and etch target were precleaned at 3mTorr pressure and

Contributed by the Tribology Division for publication in the ASME JOURNAL OF TRIBOLOGY. Manuscript received by the Tribology Division December 14, 1999; revised manuscript received October 31, 2000. Associate Editor: Y.-W. Chung.

[1]Certain commercial equipment, instruments, or materials are identified in this paper in order to adequately specify the experimental procedure. Such identification does not imply recommendation or endorsement by the National Institute of Standards and Technology nor does it imply that the materials or equipment identified are necessarily the best available for the purpose.

250 Watts of RF power for 1 minute and 5 minutes, respectively. The films were deposited at 100 W deposition power at an Argon flow rate of 300 mm^3/s, corresponding to a pressure of 0.4 Pa. At this condition, the film growth rate is expected to be 0.4 nm/min $\pm$ 0.1 nm/min. The deposition time was 15 minutes, giving an expected carbon film of thickness 6 nm $\pm$ 1.5 nm. Mechanical measurement of thick films deposited under similar conditions resulted in a hardness value of 24 GPa [4]. The thin carbon surfaces had a measured advancing contact angle of 46 deg $\pm$ 2 deg against water and 43 deg $\pm$ 2 deg with methylene iodide. The surface energy can be calculated from the geometric mean approach based on the theory of fractional polarity to give a value of 59 $mJ/m^2 \pm 3$ mJ/m^2 [32]. Prior to use, the films were rinsed in heptane and placed in a UV plasma cleaner for 10 minutes to remove adsorbed organic contaminants.

II Surface Forces Measurements. A SFA with a lateral sliding attachment was used to measure the shear forces [29,30]. The SFA is a powerful tool for measuring shear forces since parameters such as area of contact and surface separation can be measured simultaneously via observation of the optical interferometric fringes [30]. The lateral sliding attachment slides two surfaces past each other while the SFA controls and/or measures the surface separation D, sliding speed v, normal load L, contact area A, and lateral shear force F. Typical values of v, L, A, and F in this study were 1 μm/s, 0 mN to 100 mN, 0 cm^2 to 10^{-3} cm^2, and 0 mN to 200 mN, respectively. The velocity and applied load have an estimated relative standard uncertainty of ± 5 percent of the measured values, whereas the friction force and contact area have an estimated relative standard uncertainty of less than ± 10 percent of the measured values.

The humidity was controlled by first purging the system with dry nitrogen. For the dry atmosphere condition, a small container filled with P_2O_5 was placed in the chamber of the SFA to extract residual moisture from the atmosphere. To achieve 33 percent humidity and 100 percent humidity, the P_2O_5 was removed and the container was filled with a saturated solution of $MgCl_2$ and water, respectively.

Three repeat measurements were run using two different samples. The surfaces were deposited with carbon at the same time and hence the deposition conditions were identical. Uncertainties of the calculated shear stress represent averages of the standard deviation of the data.

Results

Theories of the friction between surfaces were developed by many scientists including Amontons', da Vinci, and Colomb [17,32,33]. Bowden and Tabor modified Amontons' Laws of friction to include adhesion between the surfaces [17]. Generally, the friction force F can be described by a dependence on the true area of contact A_{real} and a yield stress τ_s according to

$$F = \tau_s A_{\text{real}} \tag{1}$$

and

$$\tau_s = \tau_0 + \alpha P, \tag{2}$$

where α represents the pressure dependence of the yield stress. The above equations can be combined to give

$$F = \tau_0 A_{\text{real}} + \alpha L \tag{3}$$

or

$$F/L = \mu = \alpha + \tau_0 / P, \tag{4}$$

where L = load and μ = friction coefficient. If the two surfaces are adhesive, as is the case in this experiment, then the friction is expected to depend more on the area of contact than on the load, at least for low loads. Note also that the friction coefficient is not a constant, but decreases with increasing pressure. Contributions to the friction due to plowing can also occur to give another term to Eq. (1). The plowing term is assumed to be small for this system.

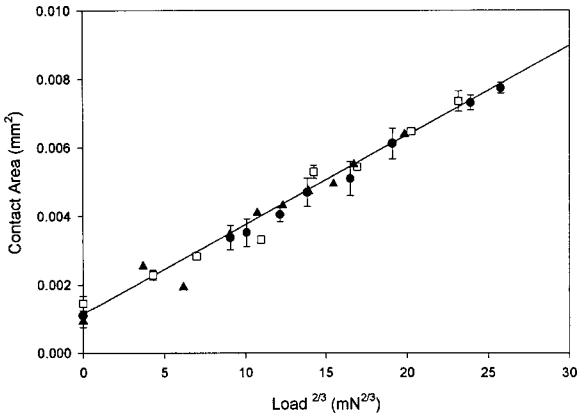

Fig. 1 Measured contact area as a function of load for sputtered carbon films on mica. The triangles, squares and circles represent measurements at 0 percent relative humidity, 33 percent relative humidity, and 100 percent relative humidity, respectively. The solid line is a least squares fit of the data. The error bars indicate estimated standard uncertainties.

The carbon surfaces used in these experiments were not perfectly smooth but had a measured degree of surface roughness. Atomic Force Microscopy (AFM) measurements of the surface topography of the carbon films gave an RMS roughness of 1 nm $\pm$ 0.2 nm for an area scan of 15 μm. Asperities as small as 2 nm in height have been shown to reduce the adhesion between dry surfaces to almost zero [34].

If the contact is elastic, it is expected to exhibit Hertzian behavior with the area of contact increasing as $L^{2/3}$.[35] The measured microscopic area of contact at 0 percent, 33 percent, and 100 percent relative humidity as a function of $L^{2/3}$ is shown in Fig. 1. The data points represent an average of two values taken at the same load while the surfaces were sliding. The solid line is a linear regression fit to the data. The error bars estimate standard uncertainties in the data for one contact position. Clearly, the area varies as $L^{2/3}$ as expected for Hertzian behavior. The contact diameter varied from 30 mm to 100 mm whereas the thicknesses of the mica and carbon overcoat were 3 mm $\pm$ 0.5 mm and 6 nm $\pm$ 1.5 nm, respectively. Because the epoxy attaching the carbon coated mica sheets to the glass substrate is relatively soft, its modulus ($E \approx 2$ GPa) is likely to dominate the measured load dependence [36]. Hence, much of the stress will be taken up by the elastic epoxy layer. This relatively soft underlayer also allows the two interacting carbon surfaces to conform, giving a larger fraction of real area of contact to measured area of contact than observed in less compliant systems. Within experimental error, no difference was observed between the measured contact area as a function of load measured in dry and humid air. The non-zero value of the contact area at no applied load demonstrates that the surfaces were adhesive. A more accurate description of the area-load dependence for the adhesive, elastic case is given by the JKR equation [35].

At 0 percent relative humidity, the surfaces initially jumped into contact under zero load giving a flattened contact area. This jump to contact shows that the surface interaction was adhesive. No attempts were made to measure the adhesion force from the jump distance by separating the surfaces since the optical interference fringes were quite faint due to the carbon coating. The surfaces initially remained pinned as a shear force was applied. Suddenly, the surfaces slipped (a few contact diameters) and again the surfaces pinned at a smaller contact diameter. The (static) shear stress

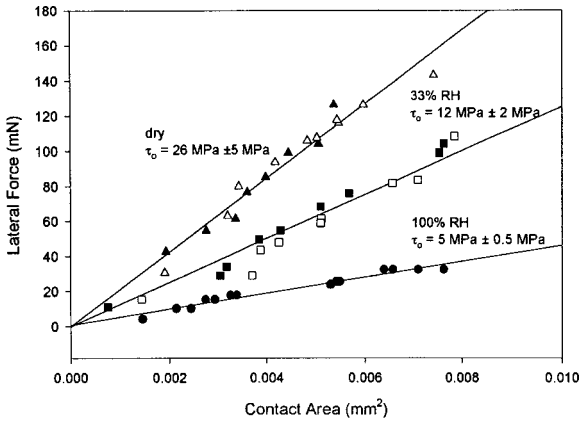

Fig. 2 Lateral Force versus contact area for sputtered carbon films on mica. The open symbols represent measurements in the forward direction whereas the closed symbols represent measurements in the reverse direction. Measurements are shown for 0 percent relative humidity (triangles), 33 percent relative humidity (squares) and 100 percent relative humidity (circles). Both the friction values and the contact areas have an estimated relative standard uncertainty of ±10 percent of the measured values. The solid line is a linear regression fit to the data. The slope of the lines give the shear stress, τ, which clearly decreases as the humidity increases.

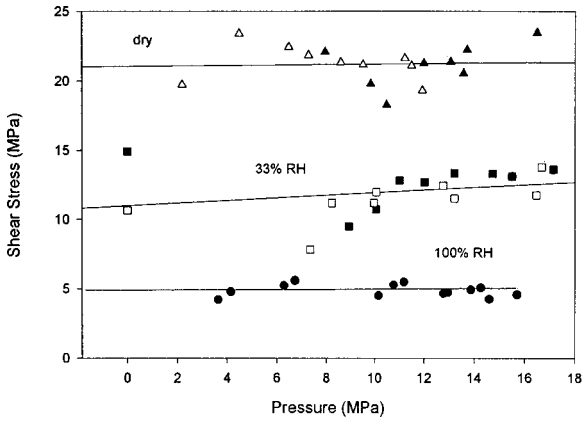

Fig. 3 Shear Stress (Friction/Area) versus pressure (Load/Area) for sputtered carbon films on mica measured at 0 percent relative humidity (triangles), 33 percent relative humidity (squares), and 100 percent relative humidity (circles). The shear stress and pressure have an estimated relative standard uncertainty of ±20 percent and ±15 percent of the measured values, respectively. The solid line is a linear regression fit to the data.

at the slip corresponded to 85 MPa±10 MPa. On reversal, a much smaller slip-stick motion was observed, with the corresponding shear stress decreasing to 50 MPa±15 MPa. After traversing the contact four times, the friction force was steady (i.e., no stick-slip motion). The static friction was now only about 5 percent higher than the kinetic friction. No wear was observed during sliding.

After the surfaces had been slid over the same contact area four times at zero load, the lateral force and contact area were measured. The sliding direction was reversed and the contact area and lateral force was again measured. The load was increased and the measurements were continued. Note that because we are reversing directions, we are measuring both the force required to initiate sliding, the static friction, and the force required to maintain sliding at the sliding speed of 1 μm/s, the kinetic friction. Once the sliding was initiated, smooth sliding was observed.

Figure 2 shows the results of the measured lateral kinetic friction force versus contact area after the surfaces had been slid over a given contact position four times. The results are shown for 0 percent, 33 percent, and 100 percent relative humidity at one contact position. The filled and unfilled symbols represent measurements in the forward and reverse directions, respectively. The solid lines are least squares fits to the data. Clearly, the lateral force is proportional to the microscopic contact area and decreases with increasing humidity. No wear was observed during sliding, although there appeared to be an initial wearing in of the contact as measured by the initial static friction forces. No hysteresis in contact area was observed on subsequent measurements, demonstrating that the contact appeared to be elastic at the experimental pressures ($\leqslant$ 20 MPa) attained in this experiment.

The corresponding shear stress values (given by the slope of the data in Fig. 2) for 0 percent, 33 percent, and 100 percent relative humidity are 21 MPa±2 MPa, 12 MPa±2 MPa, and 5 MPa±0.5 MPa, respectively. The shear stress versus pressure for the carbon-carbon surfaces is shown in Fig. 3 for each humidity level. The shear stress is independent of pressure, at least for pressures less than 20 MPa. A slightly higher shear stress was measured for carbon surfaces not previously treated by a UV cleaner. In those measurements, the shear stress was measured to be 29 MPa±2 MPa under dry conditions. Averaging the data for UV cleaned surfaces and non UV cleaned surfaces gives a shear stress of 26 MPa±5 MPa for carbon surfaces sliding in dry air.

As the humidity increases, a water film adsorbs on the surfaces. Generally, the optical interference fringes allow measurement of the intervening film thickness between the surfaces to ±0.1 nm. However, the carbon coating significantly reduced the optical signal and thus the water film thickness could not be accurately measured. Ellipsometry has been used to measure the thickness of adsorbed water films, and has shown that the thickness depends strongly on the chemistry and surface energy of the solid surface [31,37,38]. For sputtered carbon films on commercially available magnetic hard disks, the thickness of the adsorbed water film was measured to be less than 0.5 nm at relative humidities less than 85 percent [21]. The film thickness increases nonlinearly above 85 percent relative humidity to a value near 4 nm at 100 percent humidity. For pyrolytic carbon, water film thicknesses at 100 percent relative humidity have been measured to be 8 nm [37]. The thickness of the water film between two carbon surfaces may be double that for one surface, but the water could diffuse from the contact zone under an applied load.

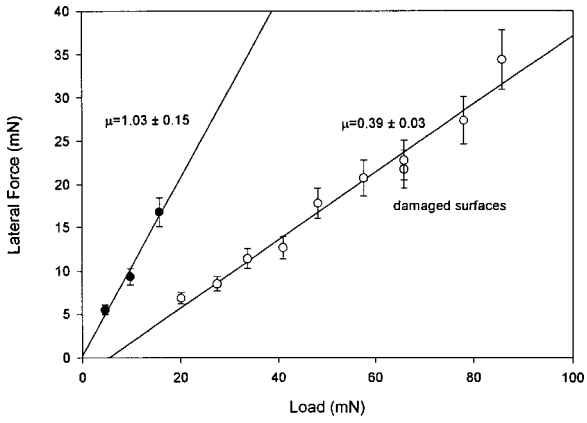

Fig. 4 Measurements of the lateral force versus applied load for one carbon coated surface sliding on one uncoated mica surface. The solid line is a least squares fit to the data. The solid circles represent measurements before the surfaces damaged, whereas the open circles represent measurements taken while sliding on wear debris. The error bars indicate estimated standard uncertainties. The damage occurred near 20 mN.

Lateral forces were also measured between dissimilar surfaces: one uncoated mica surface and one carbon coated mica surface. The measured lateral force versus load is shown in Fig. 4. At low loads ($<$20 mN) the friction coefficient ($\mu = \delta F/\delta L$) was measured to be $\mu = 1.03 \pm 0.15$. As the load was increased, damage of the surface was observed and the friction coefficient simultaneously dropped to $\mu = 0.39 \pm 0.03$. No contact areas were measured because of the difficulty in measuring the contact area in the presence of wear particles. The friction coefficient at 33 percent and 75 percent relative humidities in the presence of surface damage was measured to be $\mu = 0.29 \pm 0.02$. The corresponding measurement of the coefficient of friction for damaged uncoated mica surfaces in dry air was $\mu = 0.35 \pm 0.02$ [19].

Discussion

The friction between carbon coated surfaces in dry air can be compared to the friction previously measured between mica surfaces in dry air [19]. Mica surfaces are molecularly smooth thus eliminating any problems due to surface roughness. The shear stress τ_o measured between mica surfaces in dry air was 26 MPa$\pm$3 MPa. The shear stress measured between carbon coated surfaces in dry air was also 26 MPa$\pm$5 MPa. The surface energies, γ, of mica and carbon are quite different, $\gamma = 59$ mJ/m^2 for carbon and $\gamma = 183$ mJ/m^2 for mica [17]. Hence, the reason that the measured shear stresses in dry air are so similar between the two solids is likely due to the presence of a thin film adsorbed from air. In fact, the shear stress of a solid paraffin film is 24 MPa, indicating that the shear stress of the solid carbon and mica surfaces in air is likely due to an organic surface film adsorbed from air [39–42]. This conclusion is further supported by the measurements of the shear stress of zirconia and alumina coated mica surfaces [20]. Once again, the value of the shear strength, $\tau_o = 24$ MPa, was the same for all surfaces irrespective of the slight differences in surface roughness and surface energy. It is also interesting that the friction measured by other techniques for sputtered MoS_2 films and DLC films measured in dry air gives a shear strength of 25 MPa [18].

The presence of oxide or organic films adsorbed from air onto solid surfaces is well documented [17,37–42]. Even at the molecular level, adsorbed molecules may play an important role in the value of the measured friction [41]. The only way to completely avoid the complication of surface adsorption is to work in vacuum. For many industrial problems, this solution is not feasible. We cleaned the surfaces with a heptane rinse and uv plasma treatment immediately before use to minimize contamination. This treatment resulted in a decrease in shear stress for the uv treated surfaces, indicating that the organic layer was minimized.

The average peak-to-valley roughness between the alumina, zirconia, and carbon coated surfaces previously mentioned were 0.5 nm, 0.7 nm and 1 nm, respectively [20]. The fact that the shear stress between molecularly smooth mica surfaces is the same as that between the rougher surfaces also indicates that the microscopic surface area measured by the optical interference (FECO) fringes is quite close to the molecular contact area, presumably due to the ability of the surfaces to conform due to the soft epoxy attaching the thin mica coated sheets to the glass substrates.

A direct relationship is believed to exist between adhesion and friction [42,43]. As the adhesion increases, friction increases. Therefore, we will briefly examine the forces involved in the adhesion between surfaces [44]. For a more comprehensive investigation of the adhesive forces present between a carbon surface and a slider surface, see the work of Gui and Marchon [45].

The adhesive properties of the surfaces can be sensitive to the presence of moisture in the atmosphere. This dependence is mostly due to the capillary condensation of water around the points of contact which acts to increase the applied load between the surfaces [31,44,46]. At equilibrium, the curvature of the capillary meniscus around one spherical contact point is related to the relative humidity p/p_s by the Kelvin equation [31,44,46]:

$$\left(\frac{1}{r_1} + \frac{1}{r_2}\right)^{-1} = r_k = \frac{\gamma V}{RT \log(p/p_s)}, \tag{5}$$

where r_1 and r_2 are the radii of curvature of the meniscus, r_k is the Kelvin radius of the contact, V is the molar volume and γ is the surface tension of water. At 33 percent and 75 percent relative humidity, the Kelvin radius can be calculated from Eq. (5) to be -1 nm and -4 nm, respectively. The number is negative since the curvature is negative, giving a strong force pulling the surfaces together. Once r_K exceeds the asperity size, the adhesion force F attains its full strength given by [43,44,46]:

$$F = 4\pi R(\gamma_L \cos\theta + \gamma_{SL}), \tag{6}$$

where R is the macroscopic radius of the surface, γ_L is the surface tension of water, and γ_{SL} is the solid-liquid surface energy. The first term represents the Laplace pressure contribution to the adhesion force whereas the second term represents the solid-solid interaction. The solid-solid force contribution is often negligible, due to weak or repulsive forces occurring between the surfaces in the presence of a water film. For ceramic materials, the asperities are generally angular, not spherical, and the interaction will be slightly modified [47]. For the experiments reported here, $R = 1.5$ cm, and thus the adhesion force due to the Laplace pressure is approximately $F = 13$ mN. This force is a small fraction of the load applied to the system ($\leqslant$100 mN), and hence the decrease in the friction force with increasing humidities cannot be accounted for only by considering a decrease in the adhesive force.

The changes with humidity of the friction between carbon coated surfaces can be compared to the friction previously measured between mica surfaces [19,20]. At 0 percent, 33 percent, 75 percent, and 100 percent relative humidities, the shear stress τ_o measured between uncoated mica surfaces was 29 MPa, 17 MPa, 6 MPa, and 2 MPa, respectively. Note that the shear stress decreased by an order of magnitude as the relative humidity increased from 0 percent to 100 percent. A thin (0.3 nm to 0.6 nm) water film separated the mica surfaces in humid air. At relative humidities greater than 75 percent, trapped water lenses also could be seen between the surfaces. The water lenses were 2.8 nm$\pm$0.2 nm thick and decreased the effective area of solid-solid contact. This reduced contact area would cause a decrease in the measured friction forces, as was observed. Also, the water film separated the surfaces which decreased the friction. Hence, water acts as a good lubricant between the mica surfaces.

The carbon coated surfaces reported in this paper showed similar friction behavior to the uncoated mica surfaces. Between both mica and carbon coated surfaces, the friction and shear stress decrease with increasing vapor pressure. The shear stress at 0 percent, 33 percent, and 100 percent relative humidity was measured to be 26 MPa$\pm$5 MPa, 12 MPa$\pm$2 MPa, and 5 MPa$\pm$0.5 MPa. AT 0 percent relative humidity, similar shear stress was measured for both mica and carbon coated surfaces. At 100 percent relative humidity, the shear stress for carbon coated surfaces was about double that for mica surfaces, indicating a stronger influence of the water for the more hydrophilic mica surface than the more hydrophobic carbon surface.

Atomic Force Microscopy (AFM) measurements of silicon oxide and carbon surfaces have shown that the friction coefficient decreases with increasing humidity for silicon oxide but not for carbon [27]. The difference in the results between the AFM and the SFA experiments is likely due to the small contact diameters used for the AFM experiments compared to the SFA experiments. The larger contact area of the SFA can trap more of the adsorbed water molecules between the surfaces. A decrease in adhesive forces was observed with increasing humidity for the AFM, as expected due to the increasing Kelvin radius.

In most experimental techniques, it is the friction coefficient and not the shear stress which is readily measured (since the microscopic area of contact is not measurable in most experiments). A comparison between different techniques is especially problem-

atic because the presence of adsorbed materials on the carbon surface as well as the chemistry of the carbon dictates the frictional behavior. For the experiments reported here, a friction coefficient of 1.0 ± 0.3 was measured for a carbon surface sliding against a carbon surface in dry air. This friction coefficient is high, but not unexpected, since the applied pressures were low (<20 MPa). Because the shear stress remained independent of pressure, the friction coefficient must decrease with increasing pressure, as is observed. Other experiments are typically run at higher loads (>100 MPa) and hence the friction coefficient that is measured is much lower (typical friction coefficients for DLC carbon are 0.02 to 0.2) [8,17,18]. It is clear from previous experiments at higher pressures, and those at lower pressures presented in this study, that the friction coefficient depends on pressure. Hence, it is the shear stress, and not the friction coefficient that gives a more unambiguous representation of the friction behavior.

As mentioned in the introduction, a transfer film is often produced in solid-solid lubrication [18]. The corresponding friction that is measured results from interfilm sliding between the transfer film, which can transfer to the countersurface, and the original carbon surface. Often, the transfer film is chemically distinct from the parent film. For the carbon-carbon experiments reported here, the pressures attained are relatively low ($\leqslant 20$ MPa). Since repeat measurements were highly reproducible, the development of a chemically distinct transfer film is unlikely under these conditions. For the mica-carbon experiments, damage occurred almost immediately and behavior was governed by the formation of wear debris.

Conclusions

The friction between thin carbon films coated onto mica surfaces was found to depend on the area of contact. The shear stress decreased with increasing humidity and was independent of the pressure. The shear stress at 0 percent, 33 percent, and 100 percent relative humidity was measured to be $26\,\text{MPa} \pm 5\,\text{MPa}$, $12\,\text{MPa} \pm 2\,\text{MPa}$, and $5\,\text{MPa} \pm 0.5\,\text{MPa}$, respectively. Water acts as a lubricant, decreasing the friction between the carbon surfaces. The shear stress at 0 percent relative humidity corresponds to the shear stress of a solid paraffin film, and implies that the shear is dominated by a thin adsorbed contamination layer, at least for pressures less than 20 MPa and a velocity of 1μm/s. At 100 percent relative humidity, the shear stress for carbon coated surfaces was about double that for mica surfaces, indicating a stronger influence of the water for the more hydrophilic mica surface than the more hydrophobic carbon surface. The friction between one mica and one carbon coated surfaces resulted in immediate damage and generation of wear debris.

Acknowledgments

P.M.M. would like to thank Irwin Singer, Mike Drory, Mark Robbins, and Doug Smith for insightful discussions.

References

[1] Tsai, H., and Bogy, D. B., 1987, ''Characterization of Diamond-like Carbon Films and Their Applications as Overcoats on Thin-Film Media for Magnetic Recording,'' J. Vac. Sci. Technol. A, **5**, No. 6, pp. 3287–3312.
[2] Mee, C. D., and Daniel, E. D., 1987, eds., *Magnetic Recording*, McGraw-Hill, New York.
[3] Bhushan, B., 1996, *Tribology and Mechanics of Magnetic Storage Devices*, Springer, New York.
[4] Lu, W., and Komvopoulos, K., ''Dependence of Growth and Nanomechanical Properties of Ultrathin Amorphous Carbon Films on Radio Frequency Sputtering Conditions,'' J. Appl. Phys., **86**, No. 4, pp. 2268–2277.
[5] Cho, N. H., Krishnan, K. M., Veirs, D. K., Rubin, M. D., Hopper, C. B., Bhushan, B., and Bogy, D. B., 1990, ''Chemical Structure and Physical Properties of Diamond-Like Amorphous Carbon Films Prepared by Magnetron Sputtering,'' J. Mater. Res., **5**, No. 11, pp. 2543–2554.
[6] Grill, A., Patel, V., and Meyerson, B. S., 1990, ''Optical and Tribological Properties of Heat-Treated Diamond-Like Carbon,'' J. Mater. Res., **5**, No. 11, pp. 2531–2537.
[7] Hirvonen, J.-P., Lappalainen, R., Koskinen, J., Anttila, A., Jervis, T. R., and Trkula, M., 1990, ''Tribological Characteristics of Diamond-Like Films Deposited With an Arc-Discharge Method,'' J. Mater. Res., **5**, No. 11, pp. 2524–2530.
[8] Bull, S. J., 1995, ''Tribology of Carbon Coatings: DLC, Diamond, and Beyond,'' Diamond Relat. Mater., **4**, pp. 827–836.
[9] Hay, J. L., White, R. L., Lucas, B. N., and Oliver, W. C., 1997, ''Mechanical Characterization of Ultra-Thin Hard-Disk Overcoats Using Scratch Testing and Depth-Sensing Indentation,'' *Proceedings of the Materials Research Society*.
[10] Jiang, Z., Lu, C.-J., Bogy, D. B., Bhatia, C. S., and Miyamoto, T., 1995, ''Nanotribological Characterization of Hydrogenated Carbon Films by Scanning Probe Microscopy,'' Thin Solid Films, **258**, pp. 75–81.
[11] Mathew, Mate C., 1993, ''Nanotribology Studies of Carbon Surfaces by Force Microscopy,'' Wear, **168**, pp. 17–20.
[12] Bhushan, B., and Blackman, G. S., 1991, ''Atomic Force Microscopy of Magnetic Rigid Disk and Sliders and Its Applications to Tribology,'' ASME J. Tribol., **113**, pp. 452–458.
[13] Habig, K.-H., 1995, ''Fundamentals of the Tribological Behavior of Diamond, Diamond-Like Carbon, and Cubic Boron Nitride Coatings,'' Surf. Coat. Technol., **76–77**, pp. 540–547.
[14] Erdemir, A., Switala, M., Wei, R., and Wilbur, P., 1991, ''A Tribological Investigation of the Graphite-to-Diamond-Like Behavior of Amorphous Carbon Films Ion Beam Deposited on Ceramic Substrates,'' Surf. Coat. Technol., **50**, pp. 17–23.
[15] Gardos, M. N., 1994, ''Tribology and Wear Behavior of Diamond,'' in *Synthetic Diamond: Emerging CVD Science and Technology*, Karl E. Spear and John P. Dismukes, John Wiley & Sons, Inc., New York.
[16] Bowden, F. P., Bowden, F. R. S., and Young, J. E., 1951, ''Friction of Diamond, Graphite, and Carbon and the Influence of Surface Films,'' Proc. Roy. Soc., **208**, pp. 444–455.
[17] Bowden, F. P., and Tabor, D., 1958, *The Friction and Lubrication of Solids*, Oxford Univ. Press, Oxford.
[18] Singer, I. L., 1992, ''Solid Lubrication Processes,'' in *Fundamentals of Friction: Macroscopic and Microscopic Processes*, Kluwer Academic Publishers, Boston.
[19] Homola, A. M., Israelachvili, J. N., Gee, M. L., and McGuiggan, P. M., 1989, ''Measurements of and Relation Between the Adhesion and Friction of Two Surfaces Separated by Molecularly Thin Liquid Films,'' **111**, pp. 675–682.
[20] Hirz, S. J., Homola, A. M., Hadziiannou, G., and Frank, C. W., 1992, ''Effect of Substrate on Shearing Properties of Ultrathin Polymer Films,'' Langmuir, **8**, pp. 328–333.
[21] Li, Y., Trauner, D., and Talke, F. E., 1998, ''Effect of Humidity on Stiction and Friction of the Head/Disk Interface,'' IEEE Trans. Magn., **26**, No. 5, pp. 2487–2489.
[22] Kim, D. S., Fisher, T. E., and Gallois, B., 1991, ''The Effects of Oxygen and Humidity on Friction and Wear of Diamond-Like Carbon Films,'' Surf. Coat. Technol., **49**, p. 537.
[23] Schulz, K. J., and Viswanathan, K. V., 1991, ''A Comparison of Film Structure and Surface Chemistry of Carbon and Oxide Disk Overcoats,'' IEEE Trans. Magn., **27**, No. 6, pp. 5166–5168.
[24] Ramirez, A. G., and Sinclair, R., 1999, ''Wear-Induced Modifications of Amorphous Carbon in the Presence of Magnetic Media,'' J. Appl. Phys., **85**, No. 8, pp. 5597–5599.
[25] Enke, K., Dimigen, H., Hübsch, H., 1980, ''Frictional Properties of Diamond-like Carbon Layers,'' Appl. Phys. Lett., **36**, No. 4, pp. 291–292.
[26] Jahanmir, S., Deckman, D. E., Ives, L. K., Feldman, A., and Farabaugh, E., 1989, ''Tribological Characteristics of Synthesized Diamond Films on Silicon Carbide,'' Wear, **133**, pp. 73–81.
[27] Binggeli, M., and Mate, C. M., 1994, ''Influence of Capillary Condensation of Water on Nanotribology Studied by Force Microscopy,'' Appl. Phys. Lett., **65**, No. 4, p. 25.
[28] Gardos, M. N., and Soriano, B. L., 1990, ''The Effect of Environment on the Tribological Properties of Polycrystalline Diamond Films,'' J. Mater. Res., **5**, No. 11, p. 2599.
[29] Israelachvili, J. N., McGuiggan, P. M., and Homola, A. M., 1988, ''Dynamic Properties of Molecularly Thin Liquid Films,'' Science, **240**, p. 189.
[30] Israelachvili, J. N., and Adams, G. E., 1978, ''Measurement of Forces Between Two Mica Surfaces in Electrolyte Solutions in the Range 0–100 nm,'' J. Chem. Faraday Trans. I, **74**, pp. 975–1001.
[31] Adamson, A. W., 1976, *Physical Chemistry of Surfaces*, 3rd ed. Wiley, New York and London.
[32] Dowson, D., 1979, *History of Tribology*, Longman, New York.
[33] Johnson, K. L., 2000, ''The Contribution of Micro/Nano-Tribology to the Interpretation of Dry Friction,'' Proc. Inst. Mech. Eng., **214**, p. 11.
[34] Pethica, J. B., 1978, Ph.D. Thesis, University of Cambridge, 1978-UK.
[35] Johnson, K. L., Kendall, K., and Roberts, A. D., 1971, ''Surface Energy and the Contact of Elastic Solids,'' Proc. R. Soc. London, Ser. A, **324**, pp. 301–313.
[36] Sridhar, I., Johnson, K. L., and Fleck, N. A., ''Adhesion Mechanics of the Surface Force Apparatus.''
[37] Tadros, M. E., Hu, P., and Adamson, A. W., 1974, ''Adsorption and Contact Angle Studies,'' J. Colloid Interface Sci., **49**, pp. 184–195.
[38] Gee, M. L., Healy, T. W., and White, L. R., 1990, J. Colloid Interface Sci., **140**, No. 2, pp. 450–465.
[39] Bailey, A. I., 1961, ''Friction and Adhesion of Clean and Contaminated Surfaces,'' J. Appl. Phys., **32**, pp. 1407–1413.

[40] Briscoe, B. J., Evans, D. C. B., and Tabor, D., 1977, J. Colloid Interface Sci., **61**, p. 9.
[41] He, G., Muser, M. H., and Robbins, M. O., 1999, ''Adsorbed Layers and the Origin of Static Friction,'' Science, **284**, pp. 1650–1652.
[42] Tabor, D., 1979, ''Adhesion and Friction,'' *The Properties of Diamond*, J. E. Field, ed., Academic Press, p. 325.
[43] McFarlane, J. S., and Tabor, D., 1950, ''Relation Between Friction and Adhesion,'' Proc. Roy Soc., **202**, pp. 244–253.
[44] Israelachvili, J. N., 1992, *Intermolecular and Surfaces Forces*, 2nd ed., Academic Press, San Diego, CA.
[45] Gui, J., and Marchon, B., 1995, ''A Stiction Model for a Head-Disk Interface of a Rigid Disk Drive,'' J. Appl. Phys., **78**, No. 6, pp. 4206–4217.
[46] Fisher, L. R., and Israelachvili, J. N., 1981, ''Direct Measurement of the Effect of Meniscus Forces on Adhesion: A Study of the Applicability of Macroscopic Thermodynamics to Microscopic Liquid Interfaces,'' Colloids Surface, **3**, pp. 303–319.
[47] Cahn, J. W., and Heady, R. B., 1970, ''Analysis of Capillary Forces in Liquid-Phase Sintering of Jagged Particles,'' J. Am. Ceram. Soc., **53**, No. 7, pp. 406–409.